1

General Principles of the Wave Concept Iterative Process

1.1. Introduction

The iterative method, which uses a wave network, is an integrated method and is not based upon electric and magnetic fields, as are, for example, Electrical Field Integral Equation (EFIE), Magnetic Field Integral Equation (MFIE), or more generally the method of moments or a combination of both fields. These are likened to the amplitudes of transverse waves, both diffracting around obstacles and those in space, termed "free space", owing to the presence of evanescent fields. However, while the method of moments appeals to so-called admittance or impedance operators, within the wave iterative method (Wave Concept Iterative Process (WCIP)), the diffraction operators are restricted, thus leading to the convergence of all iterative processes based upon this particular formalism [BAU 99].

It may be noted that, with the method of moments, the solution to the problem often entails using a restriction in the given field so as to define trial functions that constitute the basis for given solutions. This often leads to both analytical and numerical problems. In the WCIP method, field conditions are simply described on the basis of pixels which make up the entire sphere.

Chapter written by Henri BAUDRAND, Med Karim AZIZI and Mohammed TITAOUINE.

Moreover, the iterative process has a significant resemblance to that used within harmonic equilibrium [KER 75]. Within this latter process the nonlinear component behaves in a way that is described in relation to time, while the rest of the circuit is described within the frequency sphere. The operator thus functions diagonally at given frequencies. With each iteration, we therefore proceed with a Fourier transform (using a time–frequency basis) so as to approach the detailed composition of boundary conditions at the shutdown level. Moreover, when writing equations in terms of components studied over time, an inverse Fourier transform (based upon frequency–time) is used.

The WCIP approach is closely related. By simply replacing time by a coordinate and the frequency by a "spatial frequency", the operation reverts to one within the spectral sphere. Outside of the Transverse Lines Matrix (TLM) method, which also necessitates the wave concept [KRU 94], the WCIP is based upon the systematic iteration between both incident and reflected waves. The approach used in the paragraphs below is as follows: select a wave definition which is consistent with pre-existing cases, in particular within waveguides, and ensure that it has a fundamental physical significance. The iterative process will then be described in the context of several types of problems, in particular quasi-periodic structures.

The objectives of this chapter are to first set out the WCIP, showing its potential for circuit modeling, antennae and quasi-optical devices within stratified environments [BAU 99, AZI 95, AZI 96, WAN 05, RAV 04, TIT 09]. There are two advantages to this method. Firstly, the iterative process is always convergent (excepting the frequency resonating from a mechanism such as that one which is also relevant to other digital methods). Secondly, by the description of all surfaces through the use of pixels, it is not necessary to use a network describing the part of the surface corresponding to a metallic coating (or indeed to the dielectric dual), as falls within the sphere of the method of moments.

In the second part of this chapter, the WCIP is outlined. The principles of the WCIP are adhered to. Through the use of combined equations, one is

expressed in the spatial sphere and the other in the spectral sphere (also called the modal sphere). The solution is obtained by achieving equilibrium between these two spheres. The description of a given mechanism is not set by rectangular pixels but by cells restricted by periodic barriers, each containing periodic non-configured sources. The sources are described within the spectral sphere (defined by periodic barriers). They are called "auxiliary sources", as they need to be substituted by impedances alone or indeed other sources or impedances, the latter being defined by each cell. Hence the use of the term spatial domain and the adjective quasi-periodic being applied to the system. This concept makes it possible to study a large variety of systems, in particular Substrate Integrated Circuits (SIC), which have been successfully developed for several years, as shown by the results from a number of examples.

The last part of the chapter provides a gateway to other interesting applications in the field of non-homogeneous meta-materials, in the sense that both sources and obstacles are integrated in a unique model, thus avoiding the use of the approximation of equivalent environments. Up until now (except for using three-dimensional simulators such as EF and Finite-Difference Time-Domain (FDTD)) homogeneous meta-materials allow us to establish their equivalent index. The link between a material and a given mechanism (for example, plate antennae) presents difficulties and cannot be approached from any perspective other than a comprehensive analysis.

Finally, we provide an overview of another WCIP-based field; the study of quasi-periodic circuits with identified components. There are many applications for these types of structures, filters, amplifiers, percolation problems and quasi-optic planar sources.

1.2. The iterative wave method

The integral form of waves came to be explained during the 1990s, and was applied to planar circuits and to antennae [BAU 99, AZI 95, AZI 96, WAN 05, RAV 04, TIT 09]. The wave concept principle is as follows:

– The electromagnetic issue may be expressed by the relationship between the two environments. The first is known as the spectral sphere or

the external environment. The second is a set of surfaces which are defined by the boundary conditions at each point (termed the spatial domain). An Ao source in the spatial sphere sends a wave with an Ao amplitude towards a vacuum of free space. This wave is partly reflected (by the reaction of the operator Γ) and provides a wave B. The latter is, in its turn, reflected within the spatial sphere (the Operator S) giving us the wave A.

– The Γ operator is diagonal within the spectral sphere. It represents the homogeneous environment and its interaction with electromagnetic waves [BAU 99]. The operator S describes the boundary conditions of the interface. It is expressed within the spatial sphere. The Fourier transform and its converse, the inverse Fourier transform, ensure the passage between both spheres. The relationships between incident and reflective waves are written as shown in [1.1] and [1.2].

$$B = \Gamma A \qquad [1.1]$$

$$A = SB + A_0 \qquad [1.2]$$

With the first iteration, the spatial sphere equation should be expressed simply as Ao ($B = 0$). B now appears with the operator Γ ($B = \Gamma A$). The equation [1.2] is applied so as to obtain the new value of A placed within [1.1], resulting in the new B value. This iterative process consists in successively applying equations [1.1] and [1.2], until convergence occurs (Figure 1.1).

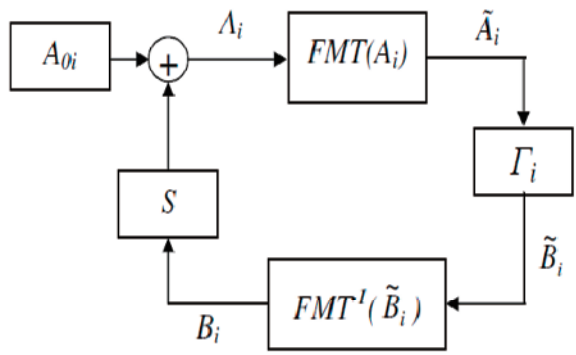

Figure 1.1. *Iterative wave diagram*

For a planar circuit within a rectangular housing, the operator Γ is diagonal across modes TE and TM, as are both the rapid transformation in methods Fast mode transform (FMT) and the opposing linking equations [1.1] and [1.2], this occurs because the operator S is diagonal in the spatial domain.

1.3. General definition of waves

The general definition of waves must meet certain conditions:

The existence of a division of the overall sphere into two sub-spheres: the internal sphere or the spatial sphere (these are flat interfaces or localized elements, indeed centers of boundary conditions within integrated methods). The second sphere is the external sphere (or spectral sphere). This sphere is most often described on the basis of the unique functions of the Helmholtz operator, which stems from Maxwell's equations. To develop this method, we need to define two dual variables such as Current–Voltage, Electric field–Magnetic field, Current density (density or surface)–Electric field, and Voltage–Load density or Voltage–Load. All of the possibilities are shown in Table 1.1. E and J may be taken as two dual variables. J is not necessarily a current-related density, but encompasses all magnitudes which are defined in Table 1.1. J may also be related to current volume density. One would thus write it as Jv to avoid confusion with the magnetic field rotated by 90°(H^n). Wave amplitudes A and B are thus defined (it may be observed that A and B may be scalars or vectors):

$$\vec{A} = \frac{1}{2\sqrt{Z_0}}\left(\vec{E} + Z_0\vec{J}\right) \qquad [1.3]$$

$$\vec{B} = \frac{1}{2\sqrt{Z_0}}\left(\vec{E} - Z_0\vec{J}\right) \qquad [1.4]$$

1.4. Application to planar circuits

The first and most frequent wave representation is where dual variables are tangential components of fields on a surface S (Figure 1.2) adjusted to account for the magnetic field by H^n (the vector product is chosen rather than the magnetic field, simply for reasons of homogeneity). This

representation is highly useful when dealing with circuits and planar antennae, frequency-selective surfaces, diffraction issues and systems involving cylindrical or spherical coordinates.

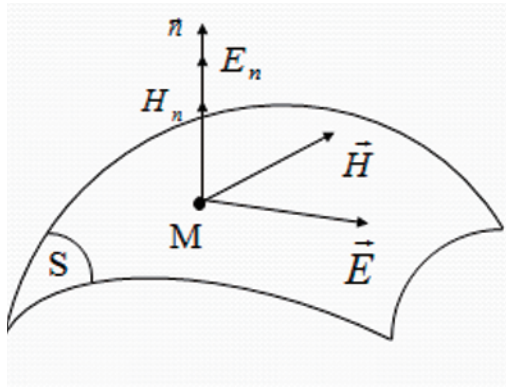

Figure 1.2. *Features of half-spaces*

1.5. Applications to quasi-periodic structures

Other types of new applications have been introduced as so-called "quasi-periodic structures". These use other wave definitions (see Table 1.1) which have applications in planar reflectors, SICs, meta-materials and photonic jets.

Dual variables	*Definition domain*	*The product of dual variables*
General case $\vec{E}\ ;\ \vec{J} = \vec{H} * \vec{n}$	TM0 mode: plane xOy	$\vec{E}.\vec{J}^{*} = \left(\vec{E} \wedge \vec{H}^{*}\right)\vec{n}$
$\vec{E}\ ;\ \vec{J_s} = \vec{H}_{2T} - \vec{H}_{1T}$	Surface with surface current $\vec{J_s}$	$\vec{E}.\vec{J_s^{*}}$ Surface power density
V; I	Lumped element circuits or TEM mode	$V \times I^{*}$ Complete power
V; ρ	Volume with load ρ	ρV Electro-static energy

Table 1.1. *Possible different dual variables*

1.6. Circuits with localized components

The traditional iterative wave method involves breaking down an electromagnetic problem into two parts [BOZ 09] as follows. The propagation equation aspect within a vacuum is dealt with in its entirety, and therefore translates as a relationship with the boundaries across sphere *D*, then with the boundary conditions running across sphere *D*. It is then necessary to have dual magnitudes linked together in a vacuum and at the boundaries, by linear operators, through a proportionality relationship (which is internal to *D*) and an integral relationship (which is external to *D*).

Figure 1.3 shows the unidimensional structure which is made up of several cells, each enclosed by periodic walls. This structure is periodic, except at source level.

$$E_2 = E_1 e^{j\alpha};\ E_3 = E_2 e^{j\alpha};\ E_4 = E_3 e^{j\alpha};\ E_5 = E_4 e^{j\alpha}$$

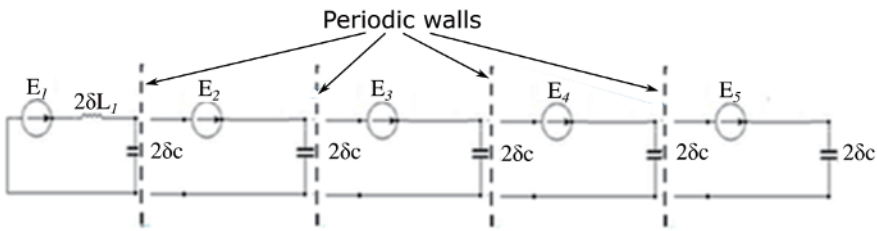

Figure 1.3. *Quasi-periodic univariate structure*

1.7. General principles of quasi-periodic circuits

Within a periodic cell-based structure, each cell is assumed to have a source. Any default at the cell level may be represented by replacing the source of the latter by impedances [WAH 92]. The structure then becomes quasi-periodic. This approach is well adapted to the iterative wave method, which acts as a balance between spectral (exterior) and spatial (internal or source) sphere, since it describes periodic geometry (external) with small spatial irregularities (the so-called sphere of sources).

One example which is often studied relates to Substrate Integrated Circuits (SICs) within an elementary cell made up of a metal or dielectric rod, which is plated by periodic walls (Figure 1.4) [BAU 09].

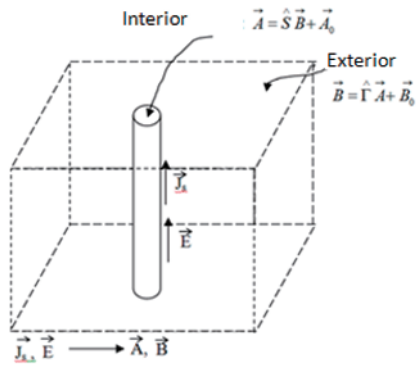

Figure 1.4. *The elementary cell*

1.8. The significance of using auxiliary sources

Consider an electromagnetic environment (Figure 1.5) comprised of one (or several) components whose behavior is described in the system V-I, E-J or even E-Js.

This element may be replaced by a source, the shutdown for which is formed by the electromagnetic environment.

The closed matrix may be established across two given sources; E_0 being the device power source and E_A being the auxiliary source.

As Figure 1.5 shows, this component may be replaced with a source (stage 1), the shutdown for which may be constituted by this component (stage 2).

The calculation produces impedance (and the potential source) in view of this source, from the electromagnetic environment. This will operate within the spectral domain.

Stage (2) involves stating that the source of stage (1) (the arbitrary source) is shutdown on the impedance of the output circuit.

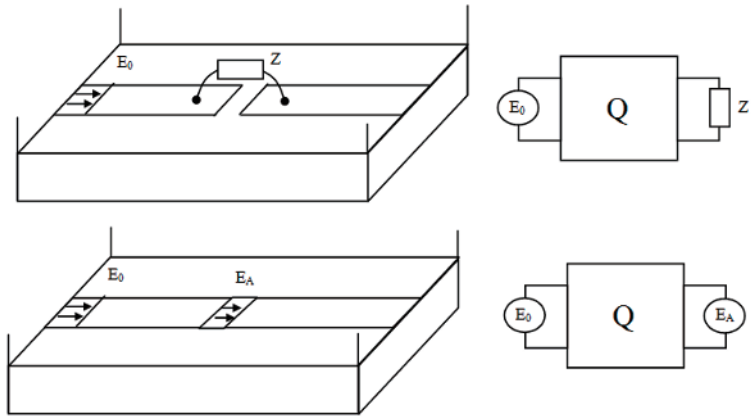

Figure 1.5. *Use of an auxiliary source*

1.8.1. *Description of the environment*

This consists of a system Q, both fed by a source S_0 and closed by an impedance Z. In general Q constitutes the center of the electromagnetic field E.M. To examine this system, we can break it down into two parts, each separate and distinct from the other and fed by a source known as the auxiliary source. System (I) describes the behavior of the impedance Z. System (II) describes the main source within its environment; E.M.Z can generally be defined at any point, and forms the spatial sphere. On the other hand, Q is often described within the environment E.M. Q is defined by its impedance or diffraction matrix. It is necessary to resort to the spectral sphere. Using this method, the calculation of impedance from the angle of S_0 is not achieved directly but it is first necessary to calculate a quadrupole with the help of an auxiliary source. This will subsequently be replaced by the localized impedance within the actual issue (allowing for its potential source). This latter operation is known as an operation in the spectral domain.

1.9. Unidimensional circuits

The configuration in Figure 1.6 shows the unidimensional structure, which is made up of several cells.

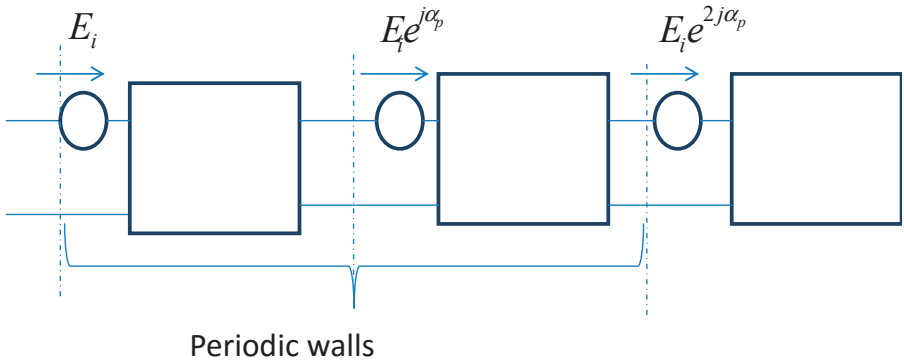

Figure 1.6. *Quasi-periodic unidimensional circuits in the state αp*

The term unidimensional circuits refers to the balanced elementary cell (Figure 1.7) plated with periodic walls.

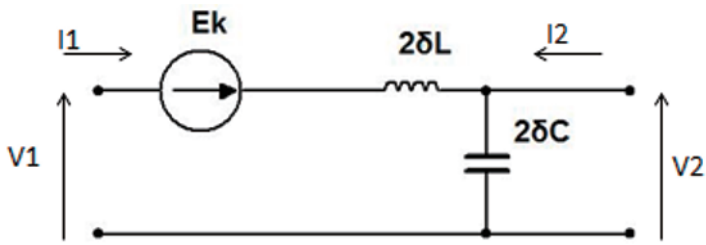

Figure 1.7. *The elementary cell*

It is first necessary to calculate the self-inductance values and the capacity for a 3 Ghz frequency. For a cell with a length δl, the capacity is $2\delta C$ and the self-inductance is $2\delta L$, hence by unit of length the formulae:

$$\delta C = 0.67.10^{-10} \ ^{*}1.25.10^{-3} = 0.84.10^{-13} F$$
$$\delta L = 1.67.10^{-7} \ ^{*}1.25.10^{-3} = 2.09.10^{-10} H$$

$$\delta L \text{ represents inductance by unit of length}$$
$$\delta C \text{ represents capacity by unit of length} \qquad [1.5]$$

The study of the structure of an artificial line made up of 100 cells at a frequency F will be completed for a given cell length $\delta l = \lambda / 40 = 2.5\ mm$. Upon isolation of the elementary cell within the unidimensional structure (Figure 1.7), all of the work which will be completed upon this cell then takes account of the periodicity walls surrounding it. This amounts to a saving both in terms of the time taken to complete the calculation, and also precision. Within the state α we must calculate $Z\alpha$ and three relationships thus arise: by taking the elementary cell in (Figure 1.7), Kirchoff's mesh and junction rules (respectively relating to voltage and current) allow us to express the following formulae:

$$V_1 + jl\omega I_1 + E_e + jl\omega I_1 = V_2 \qquad [1.6]$$

$$I_2 = -I_1 e^{j\alpha} \qquad [1.7]$$

$$I_1 e^{j\alpha} + I_1 + j\omega c V_1 e^{j\alpha} = 0 \qquad [1.8]$$

The transition from one cell to another takes place through a phase difference α, each cell being limited by periodic walls, with periodic conditions implying a phase difference between [1.1] and [1.2]. We thus get the formula:

$$V_2 = V_1 e^{j\alpha} \qquad [1.9]$$

$$\text{Thus, } V_1 + jl\omega I_1 + E_e + jl\omega I_1 = V_1 e^{j\alpha} \qquad [1.10]$$

The junction rule provides us with the equation:

$$I_1 - j\omega c V_2 = -I_2 \qquad [1.11]$$

Two of the last equations [1.7] and [1.8] of this sequence give us:

$$(j\omega c V_1 - I_1) e^{j\alpha} + I_1 + j\omega c V_1 e^{j\alpha} = 0 \qquad [1.12]$$

Hence:

$$V_1 = \frac{e^{j\alpha} - 1}{2 j\omega c e^{j\alpha}} I_1 \qquad [1.13]$$

By substituting the second equation for the first, we arrive at:

$$E = -2jl\omega I_1 + \frac{(e^{j\alpha} - 1)}{2j\omega c e^{j\alpha}} I_1 \qquad [1.14]$$

From this impedance, we deduce the result Γ_α and substitute α (a phase difference between one cell and another) by its value $\alpha = 2\pi p / N$.

Hence, the value known as spectral Γ:

$$\Gamma = \frac{Z_\alpha - Z_0}{Z_\alpha + Z_0} \qquad [1.15]$$

For the spatial sphere, we make the structure anti-symmetric (Figure 1.8). D is now equal to double the length of the line. To achieve a line of three cells requires an inductance $2\delta L$ and a capacitance of $2\delta C$, each having a dimension dl according to the wavelength λ commensurate with given requirements.

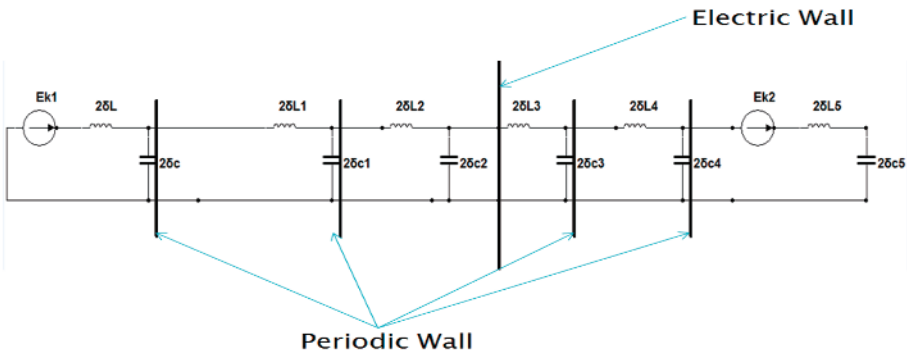

Figure 1.8. *Dividing up the cell configuration (three cells including periodic walls)*

In order to calculate S within the spatial sphere, we have to return to the initial diagram to calculate the parameters of the matrix S at source level. The transmission line acknowledges as the entry impedance Z_0 and a single

source in terms of the first cell E_{k1}. For the remainder of the cells, the sources are short-circuited.

This structure allows us to express the formula:

$$E = \begin{pmatrix} E_{k1} \\ 0 \\ 0 \\ 0 \\ 0 \\ 0 \end{pmatrix} + \begin{pmatrix} -Z_0 I_{N/2} \\ 0 \\ 0 \\ 0 \\ 0 \\ 0 \end{pmatrix} \qquad [1.16]$$

E represents the electric field.

This occurs by using both equations governing the iterative method and by substituting E in these equations below:

$$\begin{cases} A = \dfrac{1}{2\sqrt{Z_0}}(E + Z_0 \mathrm{J}) \\ \mathrm{B} = \dfrac{1}{2\sqrt{Z_0}}(E - Z_0 J) \end{cases} \qquad [1.17]$$

In terms of waves, we thus get:

$$B = \begin{pmatrix} E_{k1}/2\sqrt{Z_0} \\ 0 \\ 0 \\ 0 \\ 0 \\ 0 \end{pmatrix} + \begin{pmatrix} 0 & 0 & 0 & 0 & 0 & 0 \\ 0 & -1 & 0 & 0 & 0 & 0 \\ 0 & 0 & -1 & 0 & 0 & 0 \\ 0 & 0 & 0 & -1 & 0 & 0 \\ 0 & 0 & 0 & 0 & -1 & 0 \\ 0 & 0 & 0 & 0 & 0 & -1 \end{pmatrix} \begin{pmatrix} A_{-N/2} \\ . \\ . \\ . \\ . \\ A_{N/2-1} \end{pmatrix} \qquad [1.18]$$

This formula represents waves within the spatial domain. By doing so, we thus acknowledge equation [1.2] of the iterative method, $B = \mathrm{SA} + B_0$, as well as equation [1.15], allowing the determination of impedance within the spectral domain. Having calculated S and Γ, the current density I placed upon each cell may be determined.

1.10. Application: transmission line

Knowing the spectral Γ and the spatial S with the main sources E_1 the iterative process may be initiated and the values of I on each of the actual cells instead of auxiliary sources may be determined.

Convergence is reached after 2,800 iterations. This makes it possible to calculate the current density passing through each cell, that is to say a cell length of $\delta l = \lambda/10$.

By inserting the electric wall at the point of the 50th cell, the structure was split into two and the current density at its maximum, which allowed us to find the wavelength for 100 cells. Figure 1.10 shows current distribution for another cell length of the order of $\delta l = \lambda/50$.

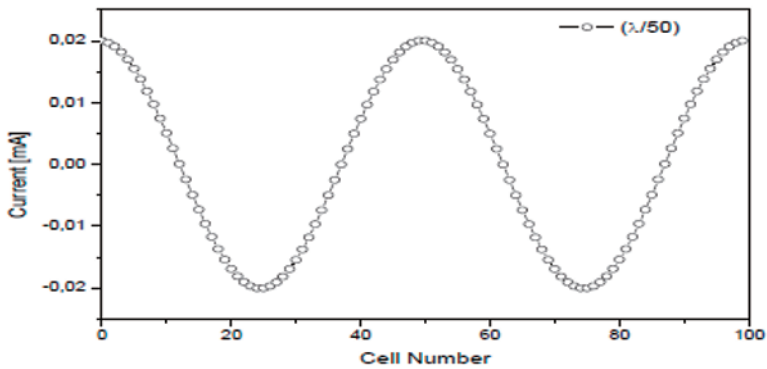

Figure 1.9. *Current according to cell number for a length λ/50*

1.11. Comparison of current density for different cell lengths

Let us now take, by way of length, the artificial line Lg = 30 cm. A simulation of this structure was completed. This thus allowed us to see the current behavior on each cell, for different cell lengths. A superimposition of three curves for current density (Figure 1.10) has been shown to see what length is most appropriate for this function.

So as to permanently fix concepts upon the choice of cell length, another length of the artificial line of the order of 15 cm was selected. This trial allows us to note that the length at which current density is stable is

$\delta l = \lambda/40$. The curve below (Figure 1.11) shows the theoretical current density component. Since it is a short circuit line, there are no losses, giving us theoretical pure impedance.

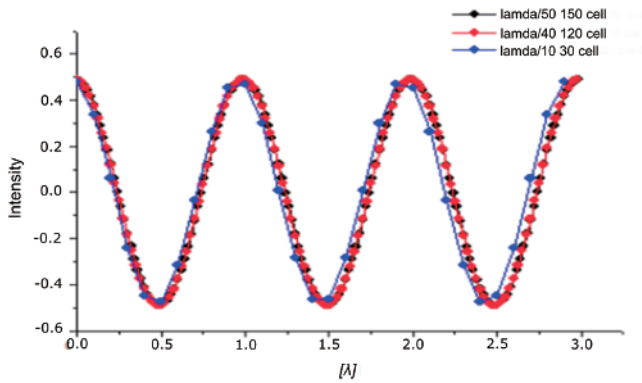

Figure 1.10. *Comparison of current density for different cell lengths for a length of 30 cm. For a color version of this figure, see www.iste.co.uk/baudrand/waves.zip*

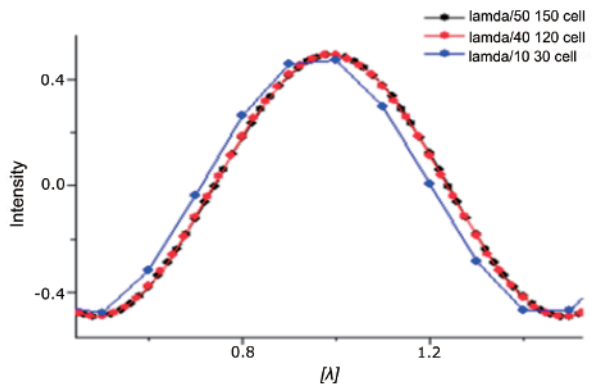

Figure 1.11. *Comparison of current density for different cell lengths measured according to wavelength λ, For a color version of this figure, see www.iste.co.uk/baudrand/waves.zip*

In the work which follows the cell length will be $\delta l = \lambda/40$, because current stability upon a cell is guaranteed for this length.

1.12. Bi-dimensional circuits

The periodic bi-dimensional structure which is made up of the cells (on the basis of N*M) will be studied. Owing to its periodicity, the elementary cell is isolated and the entire study is made up of the latter. The cell is plated by periodic walls. The transition between one cell and another takes place through two clearly established bi-directional phase differences.

1.13. Two-source bi-dimensional circuits

Figure 1.12 shows an elementary cell for detailed study.

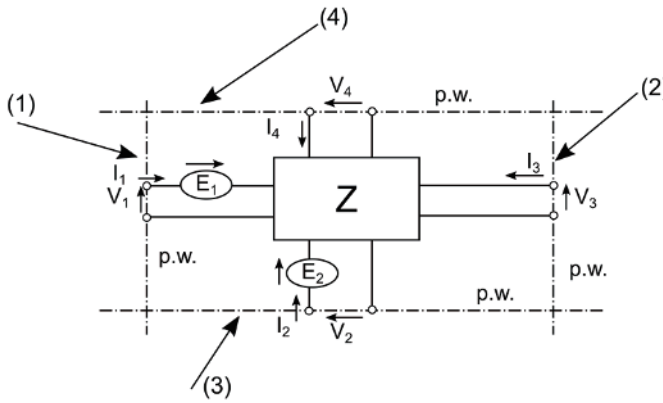

Figure 1.12. *Elementary cell*

Periodic conditions imply a phase difference between [1.1] and [1.2] and also between [1.3] and [1.4].

$$\begin{cases} V_2 = V_1 e^{j\alpha} \\ I_2 = -I_1 e^{j\alpha} \\ V_4 = V_3 e^{j\beta} \\ I_4 = -I_3 e^{j\beta} \end{cases} \qquad [1.19]$$

α and β are arbitrary. They occur because of the form, within a housing with the dimensions D*D, appreciating that the cell is of a dimension of d′*d:

$$\alpha(m) = 2\pi m \frac{d}{D} \text{ and } \beta(n) = 2\pi n \frac{d}{D} \quad [1.20]$$

Moreover:

$$\begin{vmatrix} V_1 \\ V_2 \\ V_3 \\ V_4 \end{vmatrix} = \begin{vmatrix} Z_{11} & Z_{12} \\ Z_{21} & Z_{22} \end{vmatrix} \begin{vmatrix} I_1 \\ I_2 \\ I_3 \\ I_4 \end{vmatrix} - \begin{vmatrix} E_1 \\ 0 \\ E_3 \\ 0 \end{vmatrix} \quad [1.21]$$

There are eight equations with eight unknowns:

$$\begin{vmatrix} V_1 \\ V_2 \end{vmatrix} = \begin{vmatrix} 1 \\ e^{j\alpha} \end{vmatrix} V_1 \; ; \; \begin{vmatrix} I_1 \\ I_2 \end{vmatrix} = \begin{vmatrix} 1 \\ -e^{j\alpha} \end{vmatrix} I_1 \quad [1.22]$$

$$\begin{vmatrix} V_3 \\ V_4 \end{vmatrix} = \begin{vmatrix} 1 \\ e^{j\beta} \end{vmatrix} V_3 \; ; \; \begin{vmatrix} I_3 \\ I_4 \end{vmatrix} = \begin{vmatrix} 1 \\ -e^{j\beta} \end{vmatrix} I_3 \quad [1.23]$$

By using the formula:

$$\begin{vmatrix} 1 \\ e^{j\alpha} \end{vmatrix} V_1 = Z_{11} \begin{vmatrix} 1 \\ -e^{j\alpha} \end{vmatrix} I_1 + Z_{12} \begin{vmatrix} 1 \\ -e^{j\beta} \end{vmatrix} I_3 - \begin{vmatrix} E_1 \\ 0 \end{vmatrix}$$

and [1.24]

$$\begin{vmatrix} 1 \\ e^{j\beta} \end{vmatrix} V_3 = Z_{21} \begin{vmatrix} 1 \\ -e^{j\alpha} \end{vmatrix} I_1 + Z_{22} \begin{vmatrix} 1 \\ -e^{j\beta} \end{vmatrix} I_3 - \begin{vmatrix} E_3 \\ 0 \end{vmatrix}$$

By multiplying [1.22] by $\left| e^{j\alpha}, -1 \right|$ we arrive at:

$$0 = \left| e^{j\alpha}, -1 \right| Z_{11} \begin{vmatrix} 1 \\ -e^{j\alpha} \end{vmatrix} I_1 + \left| e^{j\alpha}, -1 \right| Z_{12} \begin{vmatrix} 1 \\ -e^{j\beta} \end{vmatrix} I_3 - E_1 e^{j\alpha} \quad [1.25]$$

By multiplying [1.23] by $\left|e^{j\beta},-1\right|$ we arrive at:

$$0=\left|e^{j\beta},-1\right|Z_{21}\begin{vmatrix}1\\-e^{j\alpha}\end{vmatrix}I_1+\left|e^{j\alpha},-1\right|Z_{22}\begin{vmatrix}1\\-e^{j\beta}\end{vmatrix}I_3-E_3e^{j\beta} \qquad [1.26]$$

This brings us back to writing:

$$\begin{cases}E_1(\alpha\beta)=Z_{\alpha\beta}^{(1,1)}\,I_1(\alpha\beta)+Z_{\alpha\beta}^{(1,3)}I_3(\alpha\beta)\\ E_3(\alpha\beta)=Z_{\alpha\beta}^{(3,1)}\,I_1(\alpha\beta)+Z_{\alpha\beta}^{(3,3)}I_3(\alpha\beta)\end{cases} \qquad [1.27]$$

These relationships are described in the spectral domain, which is characterized by α and β.

The condensed form is written as:

$$\tilde{I}_{\alpha\beta}=\begin{vmatrix}I_1(\alpha\beta)\\I_3(\alpha\beta)\end{vmatrix},\quad \tilde{E}_{\alpha\beta}=\begin{vmatrix}E_1(\alpha\beta)\\E_3(\alpha\beta)\end{vmatrix}$$

The equation [1.28] is thus written as:

$$\tilde{I}_{\alpha\beta}=Y_{\alpha\beta}\tilde{E}_{\alpha\beta} \qquad [1.28]$$

Hence, it is possible to work out $\Gamma_{\alpha\beta}$.

The spatial domain corresponds to internal relationships with each source. For this, the transition by Fast Fourier transform analysis to the spectral domain is necessary.

That is to say:

$$\tilde{I}_{mn}=Y_{mn}\tilde{E}_{mn}\ \text{with}\ \alpha(\text{m})=\frac{2\pi m}{N},\beta=\frac{2\pi n}{N}\ \text{and N}=\frac{D}{d} \qquad [1.29]$$

The cells will be numbered by the integers k,l. The source phase in $k = l = 0$. The phase difference of the source k,l will be:

$$\begin{cases}k\alpha & \text{according to x}\\ l\beta & \text{according to y}\end{cases}$$

As there is an α, β phase difference during the transition from one cell to another, we may therefore write:

$$I_{kl} = \sum_{m,n} \tilde{I}_{mn} \underbrace{e^{j\frac{2\pi mk}{N}}}_{\text{phase difference with a displacement of } x} \times \underbrace{e^{j\frac{2\pi nl}{N}}}_{\text{phase difference with a displacement of y}} \quad [1.30]$$

In these conditions, $\tilde{I}_{mn}$ no longer represents the intensity of sources, but this intensity multiplied by N.

$$I_{kl=} \frac{1}{N} \sum_{m,n} \left(N\tilde{I}_{mn} \right) e^{j\frac{2\pi mk}{N}} \; e^{j\frac{2\pi nl}{N}} \quad [1.31]$$

The inverse formula for [1.31] is written as:

$$N\tilde{I}_{mn=} \frac{1}{N} \sum_{k,l} I_{kl} e^{-j\frac{2\pi mk}{N}} \; e^{-j\frac{2\pi nl}{N}} \quad [1.32]$$

The relationship in the spatial domain thus becomes:

$$I_{kl} = \underbrace{Y'_{kl}}_{\text{resistance at source level (internal impedance)}} \mathrm{E}_{kl} + \underbrace{\mathrm{I}^0_{kl}}_{\text{potential source}} \quad [1.33]$$

The spatial relationship

$$\tilde{I}_{mn} = Y_{mn} \tilde{E}_{mn} \quad [1.34]$$

Hence, the formula in waves being:

$$B = SA + B_0 \quad \text{(Spatial)}$$

$$\mathrm{A}=\hat{\Gamma}B \quad \text{(Spectral)}$$

The iterative process breaks down the problem into two parts, one in the spatial domain and the other in the spectral sphere.

Returning to the elementary cell (Figure 1.13) surrounded by periodic walls, there are four elementary cell equations which arise:

$$\begin{cases} V_3 e^{j\beta} = V_1 e^{j\alpha} \\ I_1 e^{j\alpha} + I_3 e^{j\beta} = I_1 + I_3 \\ V_1 e^{j\alpha} - V_1 = E_1 - rI_1 \\ V_3 e^{j\beta} - V_3 = E_3 - rI_3 \end{cases} \qquad [1.35]$$

In a given case, if the Z diagonal = r, we find a conventional circuit:

$$I_1 \left(e^{j\alpha} - 1 \right) = \left(1 - e^{j\beta} \right) I_3$$

By transposing [1.1] and [1.2] within [1.3] and [1.4] into the relationship given at [1.35] we arrive at:

$$V_1 \left(e^{j\alpha} - 1 \right) = E_1 - zI_1 \qquad [1.3']$$

$$V_1 e^{j(\alpha-\beta)} \left(e^{j\beta} - 1 \right) = E_3 - z \frac{e^{j\alpha} - 1}{1 - e^{j\beta}} I_1 \qquad [1.4']$$

Transposing [1.3′] into [1.4′] gives us:

$$(E_1 - rI_1) e^{j(\alpha-\beta)} \frac{e^{j\beta} - 1}{e^{j\alpha} - 1} = E_3 + \frac{e^{j\alpha} - 1}{e^{j\beta} - 1} I_1 \qquad [1.36]$$

or

$$E_1 e^{j(\alpha-\beta)} \frac{e^{j\beta} - 1}{e^{j\alpha} - 1} - E_3 = I_1 \left(\frac{e^{j\alpha} - 1}{e^{j\beta} - 1} + e^{j(\alpha-\beta)} \frac{e^{j\beta} - 1}{e^{j\alpha} - 1} \right) \qquad [1.37]$$

that is to say:

$$a = e^{j(\alpha-\beta)}$$

$$b = \frac{e^{j\beta} - 1}{e^{j\alpha} - 1} \qquad [1.38]$$

with: $I_1 = -bI_3$

The previous relationship is written as:

$$abE_1 - E_3 = I_1\left(\frac{1}{b} + ab\right) = -I_3\left(1 + ab^2\right) \qquad [1.39]$$

Hence, the admittance matrix:

$$\begin{vmatrix} I_1 \\ I_3 \end{vmatrix} = \begin{vmatrix} \dfrac{ab^2}{1+ab^2} & \dfrac{-b}{1+ab^2} \\ -\dfrac{ab}{1+ab^2} & \dfrac{1}{1+ab^2} \end{vmatrix} \begin{vmatrix} E_1 \\ E_3 \end{vmatrix} \qquad [1.40]$$

Although it is surprising, the matrix is non-reciprocal. It would be sufficient to change the origin of the I_3 phases. To achieve this:

In setting out $I_3 = aI_3^{'}$, the relationship between current density and the magnetic field, this formula becomes:

$$\begin{vmatrix} I_1 \\ I_3' \end{vmatrix} = \begin{vmatrix} \dfrac{ab^2}{1+ab^2} & \dfrac{-b}{1+ab^2} \\ -\dfrac{b}{1+ab^2} & \dfrac{1}{a\left(1+ab^2\right)} \end{vmatrix} \begin{vmatrix} E_1 \\ E_3 \end{vmatrix} \qquad [1.41]$$

$$\begin{vmatrix} \dfrac{ab^2}{1+ab^2} & \dfrac{-b}{1+ab^2} \\ -\dfrac{b}{1+ab^2} & \dfrac{1}{a\left(1+ab^2\right)} \end{vmatrix} \text{ represents the admittance matrix } Y\alpha\beta \qquad [1.42]$$

From [1.42], the matrix $\hat{\Gamma}_{\alpha\beta}$ may be calculated by the relationship:

$$\hat{\Gamma}_{\alpha\beta} = \frac{1 - rY_{\alpha\beta}}{1 + rY_{\alpha\beta}}$$

With respect to internal relationships:

$$B = SA + B_0$$

$$S = \begin{cases} -1 \ short \ circuit \\ 1 \ open \ circuit \end{cases}$$

1.14. Three-source bi-dimensional circuits

These are as per the following description of the elementary cell with a transmission line (Figure 1.14) having the length δl, which is made up of three auxiliary sources E_1, E_3 and E_5 following the three respective directions X, Y and Z and the resistance R. The source is fed into point Z and polarized at point Y.

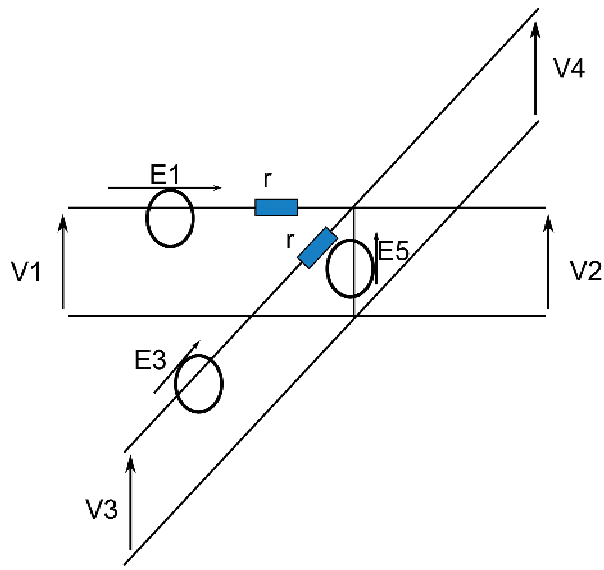

Figure 1.13. *Elementary cell with three sources E_1, E_3 and E_5*

Sources E_1, E_3 and E_5 rely upon electric walls so as to have an alternative current. If they rely upon magnetic and periodic walls the current will have a zero value.

We have eight equations and eight unknowns:

$$V_2 = V_4 = E_5 \quad [1.43]$$

$$I_1 + I_2 + I_3 + I_4 + I_5 = 0 \quad [1.44]$$

$$V_1 + E_1 - rI_1 - E_5 = 0 \quad [1.45]$$

$$V_3 + E_3 - rI_3 - E_5 = 0 \quad [1.46]$$

With the four equations for periodicity:

$$V_2 = V_1 e^{j\alpha} \quad [1.47]$$

$$I_2 = -I_1 e^{j\alpha} \quad [1.48]$$

$$V_4 = V_3 e^{j\beta} \quad [1.49]$$

$$I_4 = -I_2 e^{j\beta} \quad [1.50]$$

Upon rewriting these equations by eliminating V_2, I_2, V_4, I_4:

$$\begin{aligned} &I_1(1-e^{j\alpha}) + I_3(1-e^{j\beta}) + I_5 = 0 \\ &V_1 e^{j\alpha} = V_3 e^{j\beta} = E_5 \end{aligned} \quad [1.51]$$

$$\begin{aligned} &V_1(1-e^{j\alpha}) + E_1 - rI_1 = 0 \\ &V_3(1-e^{j\alpha}) + E_3 - rI_3 = 0 \end{aligned} \quad [1.52]$$

these two equations are written as:

$$\begin{aligned} &E_5 e^{-j\alpha}(1-e^{j\alpha}) + E_1 = rI_1 \\ &E_5 e^{-j\beta}(1-e^{j\beta}) + E_3 = rI_3 \\ &-rI_1(1-e^{j\alpha}) - rI_3(1-e^{j\beta}) = rI_5 \end{aligned} \quad [1.53]$$

That is to say:

$$a = e^{-j\alpha}(1-e^{j\alpha})$$
$$b = e^{-j\beta}(1-e^{j\beta})$$

These equations then become:

$$r\begin{vmatrix} I_1 \\ I_3 \\ I_5 \end{vmatrix} = \begin{vmatrix} 1 & 0 & a \\ 0 & 1 & b \\ a^* & b^* & |a|^2 + |b|^2 \end{vmatrix} \begin{vmatrix} E_1 \\ E_3 \\ E_5 \end{vmatrix} \quad [1.54]$$

It is now necessary to move on to the calculation of actual values so as to determine the reflection coefficient.

$$\text{Hence: } \Gamma = 1 - \frac{2\frac{Z_0}{r}}{1+\frac{Z_0}{r}} YY^+ - \frac{2\frac{Z_0}{r}(1+|a|^2+|b|^2)}{1+\frac{Z_0}{r}(1+|a|^2+|b|^2)} ZZ^+ \quad [1.55]$$

When r tends towards 0:

$$\Gamma = 1 - 2YY^+ - 2ZZ^+ \quad [1.56]$$

For the matrix S:

$$S = \begin{cases} -1 \; short \; circuit \\ 1 \; open \; circuit \end{cases}$$

Once the Γ and S parameters have been determined, the iterative process may be applied with the aid of these equations.

$$\begin{aligned} B &= \Gamma A \\ A &= SB + A_0 \end{aligned} \quad [1.57]$$

Upon achieving convergence, the field Ez may be determined across the entire structure.

To display the couplings between the cells, the transition from configuration to an activated line with a five-cell configuration, which is activated in Z (see Figure 1.14), is essential:

$$f = 3.10^9 GHz, Z_0 = 50\Omega, r = 5\Omega, \Delta l = \frac{\lambda}{10}$$

1.15. Validation examples

The structure below (Figure 1.14), is made up of 30*30 cells with a supply from the central cell (15:15) in *Y*.

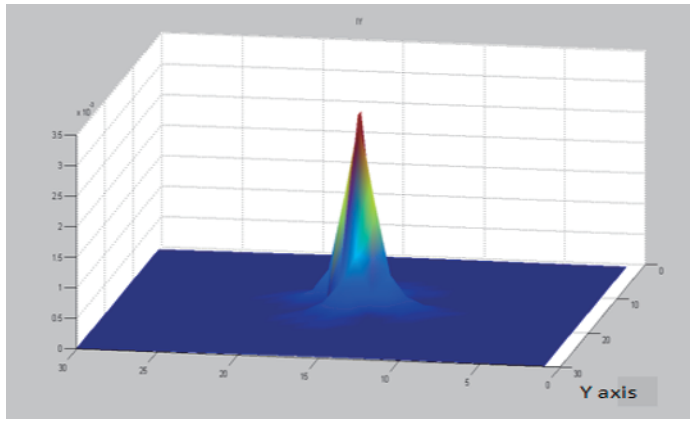

Figure 1.14. *Current density for the central cell activated in Y*

In Figure 1.15, the curve represents an emergence of the current from the central cell. The current density is of the order of 10^{-3} A/m². Across the rest of the cells the current is not, in fact, zero, but rather of the order of 10^{-5} A/m².

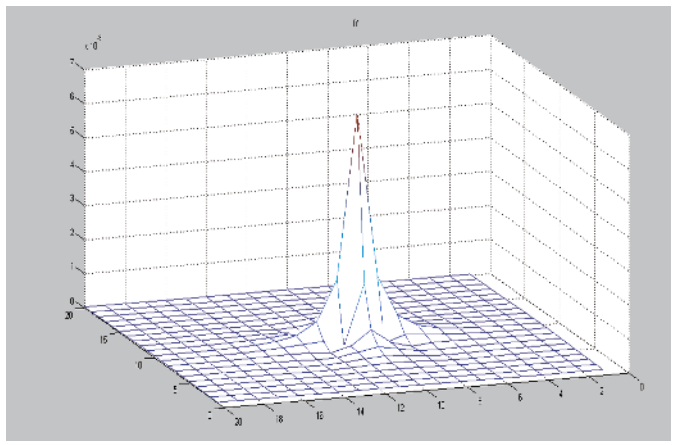

Figure 1.15. *Current density for a structure made up of 20 *20 cells with a central cell activated in Y*

This example in (Figure 1.15) demonstrates polarization in *Y*, with a source supplied in *Y* and short-circuited in *X*. The structure is 20*20 cells. The supply source is centered within a (10, 10) configuration with a current of the order of 6.65×10^{-5} A/m². A current emerges in *X* and *Y* (in Figure 1.16), since there is a coupling between *X* and *Y*.

To visualize couplings between cells, we transition from a single activated line circuit to a five-cell configuration, which is activated in *Z* (Figure 1.17).

In this configuration, for a given column of cells, these various cells are independent (in the *Y* direction), the equation being:

$$Z_L = \frac{Z_l - Z_0}{Z_l + Z_0}$$

with $Z_l = jlw$.

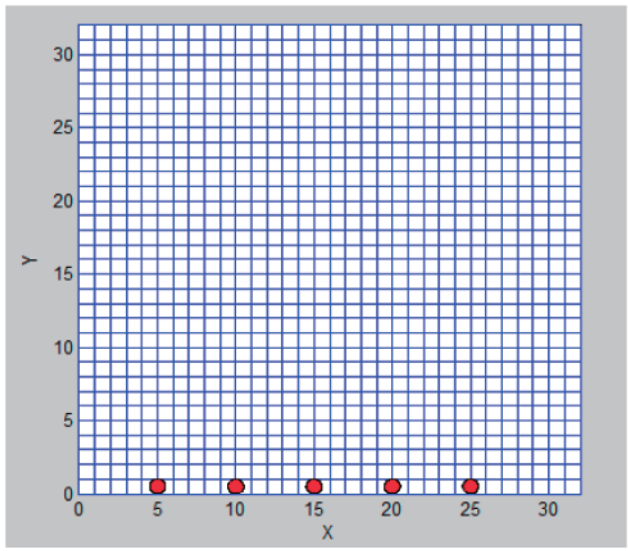

Figure 1.16. *Five-cell configuration with a source activated in Z*

The results are shown in (Figures 1.17 and 1.18). The field Ez is propagated according to the direction of polarization (*Y*) for each cell source which is fed in *Z*.

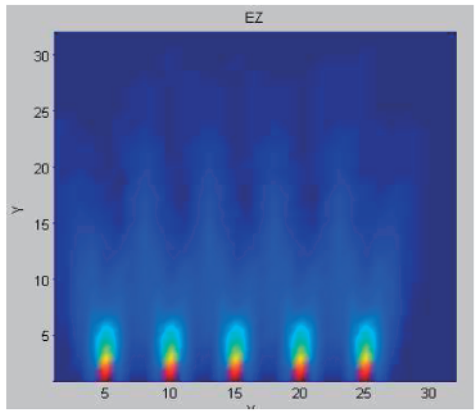

Figure 1.17. *Five-cell configuration with a source activated in Z, shown in two-dimensions*

In view of the presence of a resistance behind the auxiliary sources, the curve represents the decrease both in the magnitude of the field Ez (Figure 1.18) and the propagation following the *Y* direction.

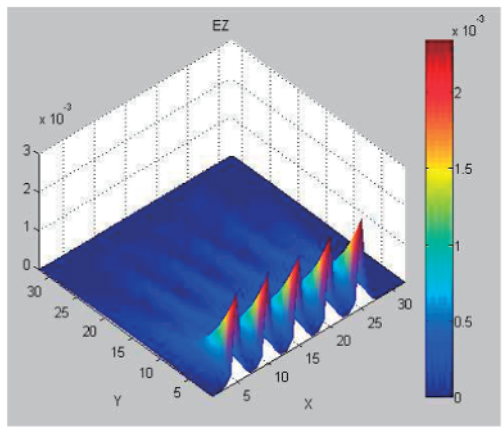

Figure 1.18. *Five-cell configuration with an activated source in Z shown in three-dimensions. For a color version of this figure, see www.iste.co.uk/baudrand/waves.zip*

That is to say, this is a bi-dimensional structure made up of 30 *30 cells, and the sources in Z on the first line are all activated. On the same line, the phase difference from one cell to another (depending upon the X direction) is of the order of $2\pi m/N$, with N being the number of cells on each line.

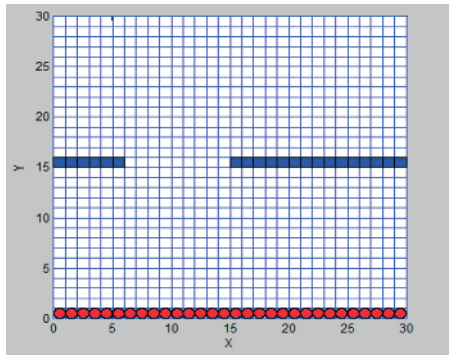

Figure 1.19. *Diagrammatic representation of the structure being studied. The source cells in red (lower line) are active and those in blue (above) are impediment cells. For a color version of this figure, see www.iste.co.uk/baudrand/waves.zip*

In this structure "impediment cells" will be inserted. These are cells covered with metal, at the 15th line, as shown in Figure 1.19. To simulate an "impediment cell", E_1 and E_3 are each replaced by an inductance and E_5 is replaced by a capacitance.

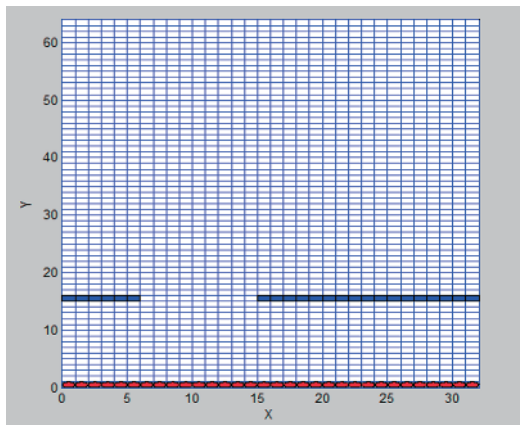

Figure 1.20. *Diagrammatic representation of the studied structure. The active source cells are in red (lower line) and the impediment cells are in blue (above). For a color version of this figure, see www.iste.co.uk/baudrand/waves.zip*

That is to say, this provides a configuration made up of 64*32 cells, each cell being of the size $dl = \lambda/20$. Our entire study revolves around a single elementary cell. The first-line sources of this structure are fed in *Z*. In *X* and *Y*, the sources are replaced by inductances known as *L*.

The impediment cells within the structure are on the 15th line. A slit was created on this line to examine the behavior of the Ez field (Figure 1.20).

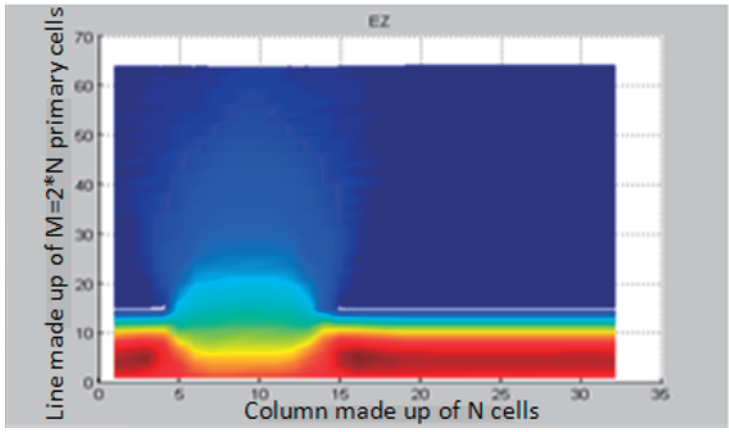

Figure 1.21. *E_z as a function of the number of cells in X and Y directions for a structure made up of 64x32 cells*

The curve shows the behavior of the density in the field Ez upon each cell, at the level of the impediments on line 15. The Ez fields are reduced while at the level of the slit, the field is propagated and this shows stationary waves.

Within the following curve (Figure 1.22), the behavior of the Ez field at the level of the 15th line is shown: being metal from 0 to 5, followed by an opening from 5 to 15, and then metal from 15 to 32.

Let us now take the same configuration previously studied and invert the cells, by replacing the cells at the slit by impediment cells (Figure 1.23). The propagation of the Ez field is shown in Figures 1.24 and 1.25.

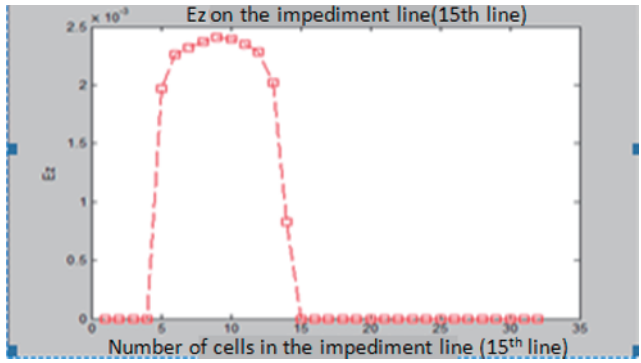

Figure 1.22. *Behavior of the E_z field on the 15th line*

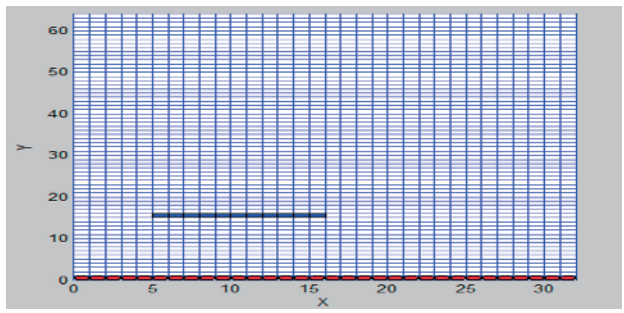

Figure 1.23. *Diagrammatic representation of the structure studied. The active source cells are shown in red (lower line) and the impediment cells are shown in blue (above). For a color version of this figure, see www.iste.co.uk/baudrand/waves.zip*

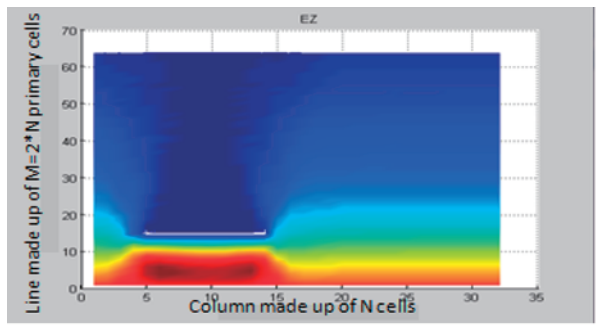

Figure 1.24. *E_z as a function of the cells number in X and Y directions for structure made up of 64 x 32 cells and shown in Figure 23. For a color version of this figure, see www.iste.co.uk/baudrand/waves.zip*

The behavior of the field Ez differs from that found within the IRIS structure; at the level of impediments on line 15 the field Ez backscatters towards the first line, but at the level of the slit for the stationary waves all along the remainder of the structure. The behavior of the Ez fields at the level of the 15th line is as follows: a gap from 0 to 5, then metal from 5 to 15, and then a gap from 15 to 32. This is shown on Figure 1.25.

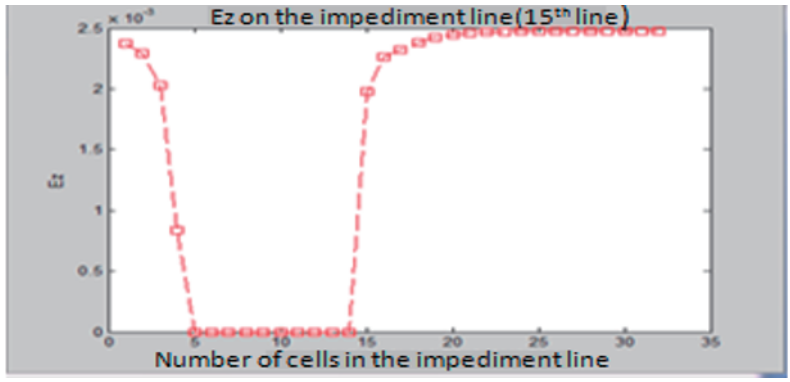

Figure 1.25. *Behavior of the E_z field on the 15th line*

The case of the central cell, the source being fed in Z

This sub-heading refers to the case of a central cell fed by a source in Z (Figure 1.26). Here, the sources within X and Y are replaced by inductances. We see the behavior of field Ez across a structure of 64 *64 cells with a cell length of the order of $\lambda/20$.

When the source in Z of the center cell is activated, the field Ez is propagated in the two directions X and Y by creating both circular and stationary waves around this same cell (Figure 1.27). The distance between each wave is of the order of 20 cells which makes it possible to find the start wavelength λ, since $dl = \lambda/20$.

Once the central cell source in Z has been activated, a symmetrical line around the propagation of Ez appears (Figure 1.28) following the x direction (the curve in red, boxes) and another symmetrical line around the propagation of Ez following y (the curve in blue, crosses) will be shown.

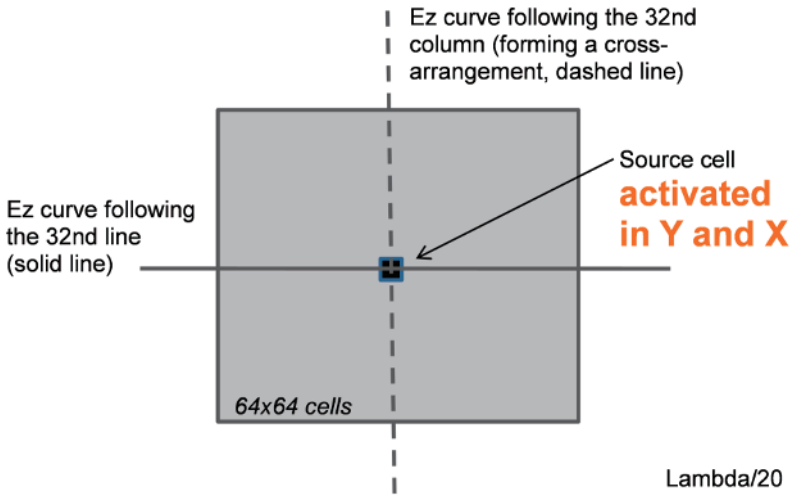

.

Figure 1.26. *Description of the configuration 64 *64 cells*

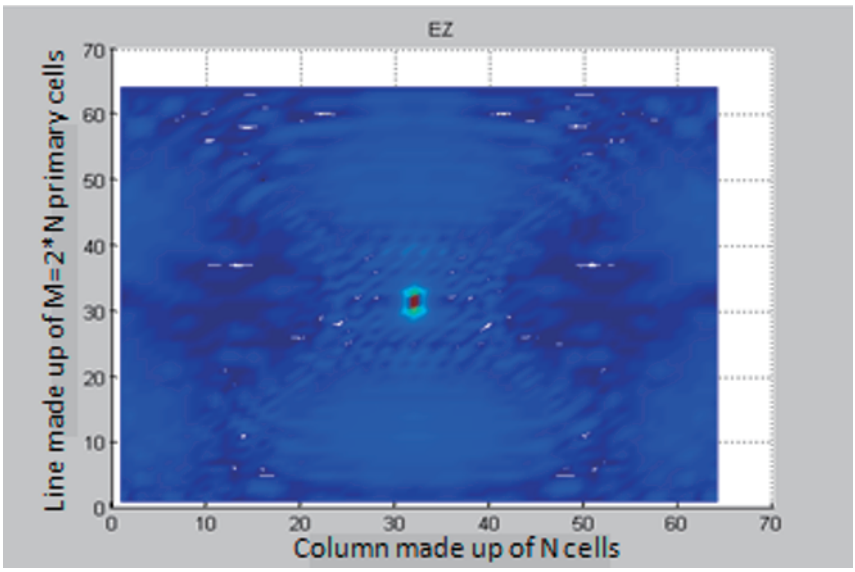

Figure 1.27. *Field E_z as a function of the cells number in X and Y directions for a structure made up of 64*64 cells and shown in Figure 1.26 with dl= λ/20*

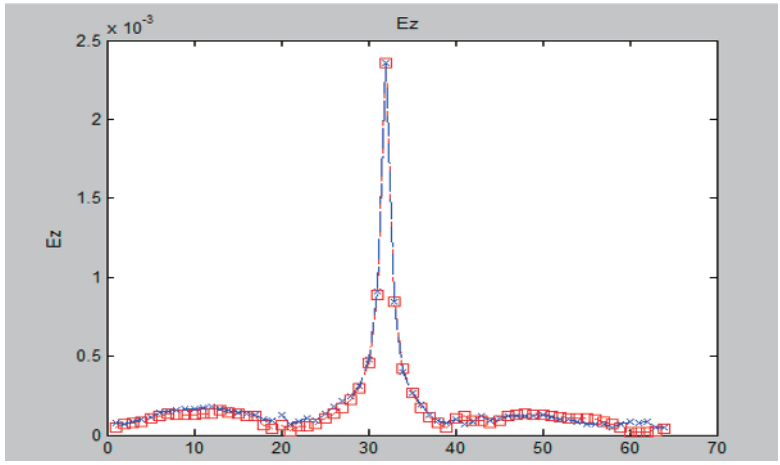

Figure 1.28. *Behavior of field Ez at the level of the central source in X (red boxes) and in Y (blue crosses). For a color version of this figure, see www.iste.co.uk/baudrand/waves.zip*

For a length $dl = \lambda/100$; this is the source that is fed in Z – the central cell. The curve shows the appearance of the field Ez (see Figure 1.29) which is propagated from the central source across the entire structure of 64 *64 cells, with a cell length of the order of $\lambda/100$.

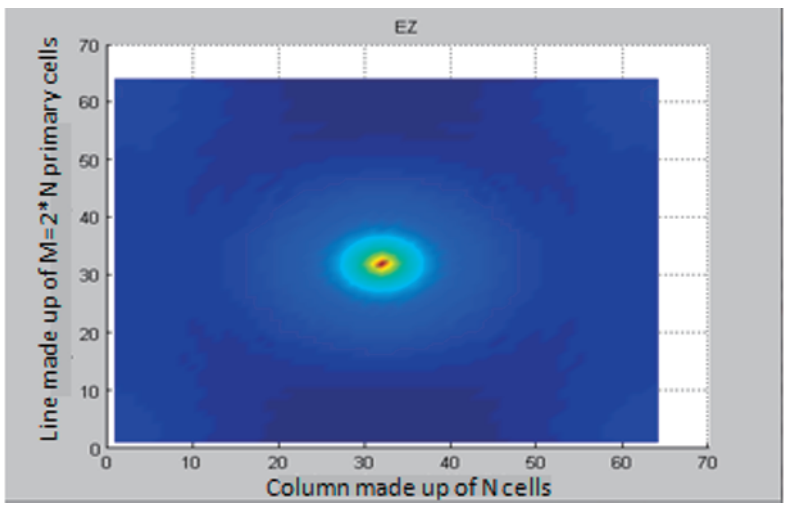

Figure 1.29. *Field E_z as a function of the number of cells in X and Y directions for a structure made up of 64*64 cells and shown in Figure 1.26 with dl= $\lambda/100$*

The validation of the study of this type of bi-dimensional configuration must undergo a comparison with studies previously completed, such as the Hankel function (Figure 1.30). This is used in applications for electromagnetic cylindrical guides, for example, within a given diffraction problem, by a cylinder which is both infinite in length and illuminated by a plane wave. The Hankel function tends towards 0 by moving away from the center.

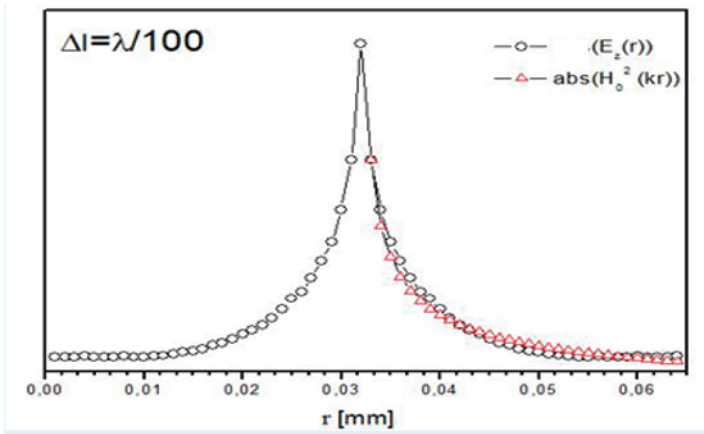

Figure 1.30. *Comparison of the Ez field's behavior for a central source which is active in Z, and the Hankel function*

The Ez field is at its maximum at the level of the central source, and decreases by being propagated along the structure in both directions *X* and *Y*. It is superimposed with the Hankel function for a cell length of the order of $\lambda/100$. This both verifies and validates the theoretical approach adopted for the study of quasi-periodic bi-dimensional structures [AZI 13].

1.16. Lenses and meta-materials

Isolating the elementary cell of the bi-dimensional structure (Figure 1.31) is necessary to calculate the values of permittivity and the corresponding permeability. The entire study of the structure takes place across

the elementary cell, viewing the periodicity of the walls surrounding the latter.

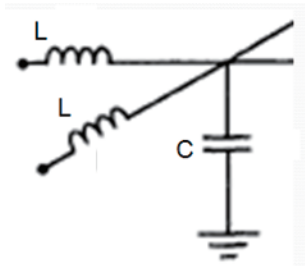

Figure 1.31. *Elementary cell*

The values of L and C determine the values of μ and ε, that is to say δl the length of the elementary cell, the capacity per unit of length is equal to:

$$C_c = C/\delta l \qquad [1.58a]$$

$$L_L = L/\delta l \qquad [1.58b]$$

and:

$$\sqrt{L_L C_C} = \sqrt{\mu_0 \varepsilon_0 \varepsilon_r} \qquad [1.58c]$$

Assuming $\mu=\mu_0$ the refraction index is given:

$$n = \sqrt{\varepsilon_r} = \sqrt{\frac{L_L C_C}{\mu_0 \varepsilon_0}} = \frac{1}{\delta l}\sqrt{\frac{LC}{\mu_0 \varepsilon_0}} = \frac{c}{\delta l}\sqrt{LC} \qquad [1.59a]$$

Where $c = 3.10^8$ m/s is the speed of light.

C_0 and L_0 are taken to be the values which lead to the formula n=1

$$\sqrt{\frac{L_0}{C_0}} = \sqrt{\frac{\mu_0}{\varepsilon_0}} \qquad [1.59b]$$

With

$$\sqrt{L_0 C_0} = \sqrt{\mu_0 \varepsilon_0}\delta l \qquad [1.59c]$$

Equation [1.59c] is extracted from the formula in [1.58c]

Multiplying [1.59b] by [1.59c] results in obtaining L_0 as:

$$L_0 = \sqrt{\frac{\mu_0}{\varepsilon_0}}\sqrt{\mu_0 \varepsilon_0}\delta l = \mu_0 \delta l \qquad [1.60a]$$

Likewise, dividing [1.59c] by [1.59b] results in obtaining C_0 as:

$$C_0 = \varepsilon_0 \delta l \qquad [1.60b]$$

On the other hand, *C* will evolve. With *n* as an index *C* becomes

$$\mathrm{C} = C_0 n^2 \qquad [1.61]$$

Conventional electrodynamics impose a resolution limit when conventional imaging uses lenses. This fundamental limit, called the "diffraction limit", in its ultimate form, is attributed to the wavelength of electromagnetic waves. The loss of resolution, which is a valid hypothesis, even if the diameter of the lens proves to be infinite, constitutes the source of the diffraction limit in its ultimate form. In the case of projecting an image from a punctual source, the diffraction limit appears as an unclear image upon a surface area of approximately a wavelength of the diameter of the lens:

$$\Delta\rho \sim 2\pi / k_0 = \lambda \qquad [1.62]$$

In 2000, John Pendry elaborated a new analysis of Veselago's lens (Figure 1.32) by introducing evanescent waves and observed that these lenses might indeed overcome the diffraction limit [PEN 99].

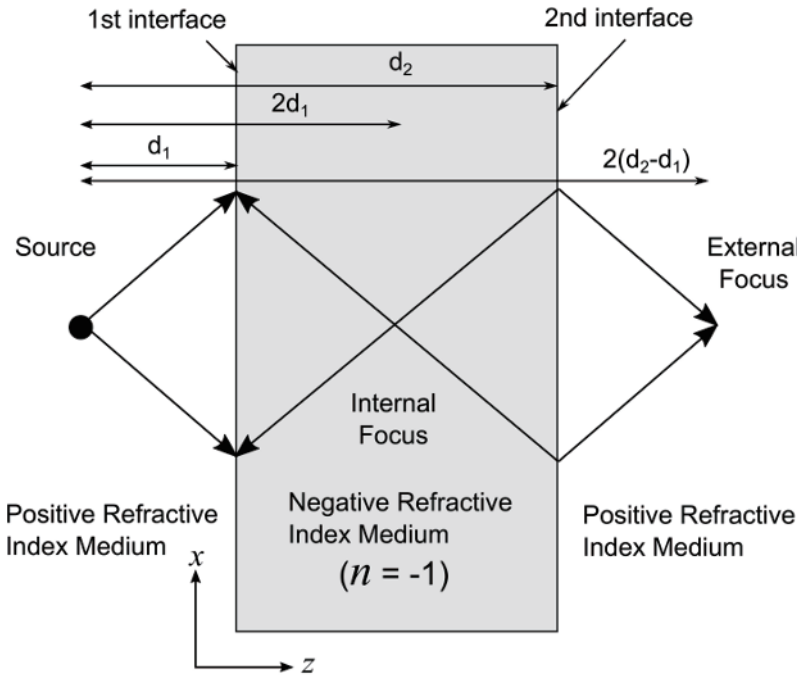

Figure 1.32. *Meta-material lens*

Pendry suggested that Veselago's lens makes it possible to have a perfect image, if it is entirely without any loss and its refractive index is exactly equal to −1 in relation to the surrounding environment. The left hand lens realizes a super-resolution image by placing the emphasis upon waves, which are propagated in the way that using a conventional lens would allow. However, it furthermore takes the amplification and restoration of evanescent waves which are splitting up and coming from the source. This restoration of evanescent waves, within the image plane extends to the numbers of maximal accessible waves, making it possible to create a very-high resolution image. The physical mechanism behind the growth of evanescent waves is somewhat interesting. Within Negative Refractive

Index (NRI) – (left-handed) materials and multiple reflections lead both to the increase and decrease of evanescent waves. Nevertheless, the index of $n = -1$ corresponds to a resonance phenomenon in which the reduction solution is canceled out, thus simply leaving the current growth of these waves.

This is achieved because when $n = -1$, the second NRI/PRI interface (Positive Refractive Index (PRI)) within Figure 1.1 corresponds to an infinite reflectance, while the first PRI/NRI interface is adjusted. In one sense, one may assimilate Veselago's lens as an inverse system which precisely restores wave propagation within free space.

An image of the plane version of Veselago's lens which was built at the University of Toronto is shown in Figure 1.33 [IYE 02]. The NRI lens is a grill structure made up of 5 × 19 cells of printed micro-strip bands, operated with series C_0 capacitors and short-circuited with an L_0 inductance. This NRI structure is sandwiched between two printed discharged grids which act as a homogeneous environment having a positive refraction index. The first non-charged network is excited using a monopole (a punctual source) which is fixed to the left-hand grid. This is reproduced by the NRI lens on the second grid. The vertical electric field across the entire structure is measured with the aid of a detection probe.

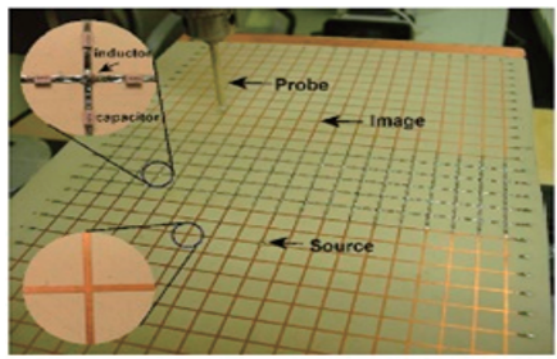

Figure 1.33. *Structure of the Veselago lens*

Meta-material cells are made up of capacitances and of self-induction coils, as shown in Figure 1.34.

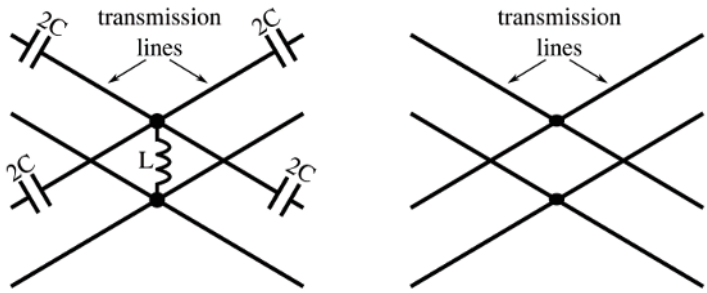

Figure 1.34. *Transmission line elementary cells*

To simulate the configuration (Figure 1.35), a source cell will be placed level with the third line at a distance from the primary interface of the meta-materials of the order $d1 = 2*d$ (that is to say corresponding with two lines of cells). The second interface [PEN 00] is placed at a distance of $2*d$ from the first interface. The source image should be focused on a distance of $2*d$ behind the second interface to validate this study [IYE 03].

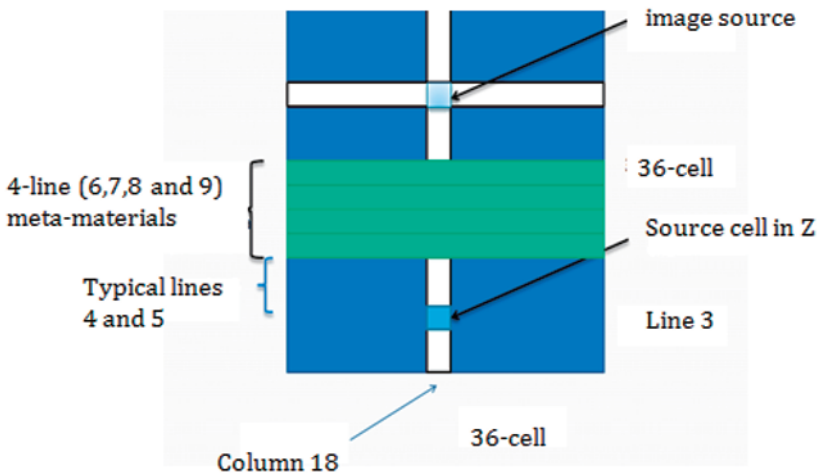

Figure 1.35. *Configuration of the lens*

Figure 1.36 shows the behavior of evanescent waves which increase within the lens. The dashed lines indicate the location of the NRI region and

the solid lines indicate the location of the source (on the top) and the external image is also given (see the view on the bottom).

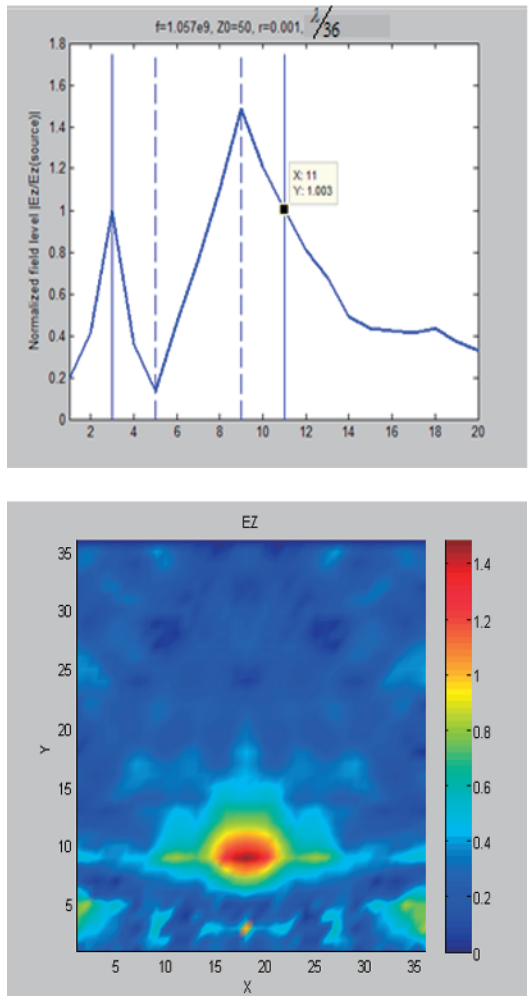

Figure 1.36. *Behavior of the field |Ez|. For a color version of this figure, see www.iste.co.uk/baudrand/waves.zip*

This thus represents an optical system which is likely to achieve a perfect image [IYE 03] of an unlimited object caused by diffraction. Negative refraction ends up forming perfect images, provided that the period of the

material is sufficiently weak when compared to wavelength. Figure 1.36 shows the principle of the super lens [GRB 04].

The elimination of the limit due to diffraction results from the amplification of evanescent waves. This amplification, which is caused by the inversion of the wave vector, makes it possible for the evanescent wave to be transmitted to the image without any reduction. To obtain this result, it is necessary for the transmission to take place without any reflection occurring upon the interfaces with the external conventional environment. If the latter consists of either air or a vacuum, with the formula $\varepsilon r = \mu r = 1$, it is therefore necessary that the left-hand material has the formula $\varepsilon r = -1$ and $\mu r = -1$.

1.17. Conclusion

We have, throughout this work, been able to trace the development of design codes and appropriate methods to deal entirely with different types of quasi-periodic structures. At the start, our objective was to both improve and broaden the scope of the WCIP iterative method within both the one-dimensional and bi-dimensional sphere. The developments introduced in the iterative method made it possible to attribute to it some qualities which are necessary to resolve propagation issues within any environment (whether homogeneous or inhomogeneous), as well as within quasi-periodic complex structures.

A study of quasi-periodic structures was made by determining the behavior of current density across each cell. In this section, we have limited the discussion to one-dimensional quasi-periodic structures. Examination of the general application of the concept of the formalism of quasi-periodic structures and the study of bi-dimensional structures was completed. When dealing with magnetic field behavior, a validation was carried out of a bi-dimensional design made up of an artificial line fitted with sources which were activated upon each cell of the structure. The last section was devoted to the study of the applications of bi-dimensional quasi-periodic configurations. Indeed, the use of the iterative method, with its novel approach with hexapole structures, has allowed us to study the so-called IRIS system as a primary application. Owing to the analogy with photonic

systems with infinite cylinders, a comparison with Hankel's function has made it possible to validate all of our work. One final application which advances the provision of the iterative method is that of the meta-material flat lens.

This work opens up a multitude of pathways. For example, the study of quasi-periodic structures based upon new materials, such as graphene, by using the WCIP method in this field appears somewhat interesting. Indeed, owing both to the exceptional properties that these materials offer and to the WCIP method, we will now be able to study the behavior of some complex structures, such as meta-surface structures, inhomogeneous structures and meta-material structures.